



## Assessment of Cytotoxicity and Genotoxicity Response of Zinc Sulphate on Eukaryotic Cells



CrossMark

Shimaa A. Mousa<sup>a\*</sup>, A. A. Haggran<sup>a</sup>, Zakia A. Abou-El-Khier<sup>b</sup>, Shadia M. Sabry<sup>b</sup> and Shimaa E. Rashad<sup>a</sup>

<sup>a</sup>Microbial Genetics Department, Biotechnology Research Institute, National Research Centre, Giza, Egypt.

<sup>b</sup>Botany and Microbiology Department, Faculty. Of Science, AL- Azhar Univ., Cairo, Egypt

### Abstract

Zinc Sulphate (ZnSO<sub>4</sub>) is an inorganic compound. Zinc is used to treat and prevent zinc deficiency. Zinc is a naturally occurring mineral that is important for growth and the development and health of body tissues. In this study, specific concentrations of ZnSO<sub>4</sub> on cell viability were investigated by MTT method in hepatocellular carcinoma (HepG2), lung cancer (A549), and normal lung cell (Wi38). Cell cycle arrest and apoptosis were measured by flow cytometry assessment by PI Staining and Annexin V/PI Staining, respectively. Results showed that Zinc induced cytotoxicity in HepG2, A549, and Wi38 using different concentrations (IC<sub>50</sub> = 308.11, 413.02, 463.15 µg/ml). These data indicated that ZnSO<sub>4</sub> decreased cell viability in malignant and non-malignant cells and confirmed the occurrence of their cytotoxic effects. Cell cycle and apoptosis by flow cytometry showed a significant increase in ZnSO<sub>4</sub>-damaged HepG2 cells by cell cycle arrest in the G<sub>2</sub>/M phase and increased apoptosis. In addition, the mRNA expression levels of p53 and casp3 increased while Bcl-2 decreased in HepG2 cell lines when treated with a high concentration of ZnSO<sub>4</sub>. The effects of ZnSO<sub>4</sub> on different yeast haploid knockout strains were evaluated in this study (YKO). We used the Comet assay method of the three different concentrations of ZnSO<sub>4</sub> at which this set of ZnSO<sub>4</sub> could cause DNA damage. The comet assay exhibited a better sensitivity of yeast cells, which was undeniably confirmed. The genotypes of YKO were chosen based on the (Clustal Omega Multiple Sequence Alignment EMBL-EBI) alignments of human and yeast gene sequence homology.

**Keywords:** Zinc Sulphate, cell lines, flow cytometry, apoptosis, RT-pcr, Comet assay.

### Introduction

Zinc is an essential trace element with important biological functions that control many processes in the cell, such as DNA synthesis, normal growth, brain development, behavioural response, fetal development and bone formation (Yehy *et al.*, 2011), regulation of response to insulin, reproduction, antioxidant cellular defense systems (Zodl *et al.*, 2003) and protein synthesis (Klug, 2010).

Zinc is effective at very low concentrations and therefore its excessive amount in body fluids could be harmful (Barbier *et al.*, 2005) Zinc is a significant trace element required for many signalling pathways in the human body by acting as a cofactor of more than 300 enzymes. These enzymes are related to the proliferation, metabolism, and functions of cells (Costello and Franklin, 2016). Furthermore, high concentrations of zinc are toxic to cells, and also, it induces a number of intracellular pathways

provoking reactive oxygen species (ROS) generation (McCord and Aizenman, 2018).

Different cell types have been exposed to Zn concentrations from 25 to 300 µM, which showed great variability in cytotoxicity and genotoxicity levels (Sliwinski *et al.*, 2009 and Plum *et al.*, 2010). Zinc deficiency results in an increased sensitivity to oxidative stress (Naziroğlu and Yürekli., 2013) and may, in part, increase the risk for cancer development (Silvera and Rohan., 2007) Excess zinc, however, can induce chromosomal instability and DNA double-strand breaks in human lung cells (Xie *et al.*, 2009).

Zaman *et al.*, 2019 demonstrate that CK2 is involved in regulating zinc homeostasis in breast and prostate cancer cells as both TBB and CX-4945 substantially decreased cell viability upon zinc exposure. Cytotoxicity and programmed cell death (apoptosis) was tested on in vitro human cell growth.

\*Corresponding author e-mail: [sa.mousa@nrc.sci.eg](mailto:sa.mousa@nrc.sci.eg); (Shimaa A. Mousa).

Receive Date: 30 May 2022; Revise Date: 07 June 2022; Accept Date: 09 June 2022.

DOI: [10.21608/ejchem.2022.141668.6209](https://doi.org/10.21608/ejchem.2022.141668.6209)

©2019 National Information and Documentation Center (NIDOC).

Cell cycle arrest and apoptosis-related genes of the human cell lines were also evaluated (**Rashad et al., 2018**).

**Rashad et al., 2019** Indicated that additives decreased cell viability in malignant and non-malignant cells as well as confirmed the occurrence of their cytotoxic effects. *Saccharomyces cerevisiae* cells were shown to be more sensitive to the action of some additives. The effects of additives on several yeast haploid knockout strains were studied in the Comet test method to find the optimum amounts at which this set of dietary additives could cause DNA damage (**Rashad et al., 2021**). AuNRs has a cytotoxic activity on human carcinoma and normal cells, Flow cytometric analysis demonstrated that AuNRs has a cytotoxic effect on human carcinoma cells (HepG2, CaCo2, A549, and CDD-19Lu) repeated through the increased G2/M phase cell cycle arrest (**Rashad et al., 2022**).

**Marcinčáková et al., 2019** evaluated the *in vitro* nephrotoxicity of zinc Sulphate heptahydrate  $ZnSO_4 \times 7H_2O$  using rabbit epithelial kidney cells RK13 as the model cell line. They reported that the inhibition concentration IC50 value for xCELLigence monitoring was 101.8 mg/l, for MTT test.

$ZnSO_4$  at a high concentration (100  $\mu M$ ) inhibited cell viability (**Zhang et al., 2017**). influences of a specific concentration range of  $ZnSO_4$  on cell cycle and apoptosis by flow cytometry, and cell viability by MTT method in MDAMB231, HepG2 and 293 T cell lines. It was found that the influence manners of  $ZnSO_4$  on cell cycle, apoptosis and cell viability in various cell lines were different and corresponding to the changes of  $Zn^{2+}$  content of the three cell lines, respectively. The significant increase on intracellular zinc content of MDAMB231 cells resulted in cell death, G1 and G2/M cell cycle arrest and increased apoptotic fraction. Additionally, the mRNA expression levels of ZnT and ZIP families in the three cell lines, when treated with high concentration of  $ZnSO_4$ , increased and decreased corresponding to their functions, respectively. The objective of this study was to assess the potential cytotoxic and apoptotic effects of  $ZnSO_4$  on human cell growth (**Wang et al., 2013**).

## Materials and methods

### 1. Cell lines

1.1. **Mammalian cell lines:** HepG-2 cells (human Hepatocellular cancer cell line), A-549 (human Lung Carcinoma) and Wi38 cells (human lung fibroblast normal cells) were obtained from the American Type Culture Collection (ATCC, Rockville, MD).

**Chemicals Used:** Dimethyl sulfoxide (DMSO), MTT and trypan blue dye were purchased from Sigma (St. Louis, Mo., USA).

Fetal Bovine serum, RPMI-1640, HEPES buffer solution, L-glutamine, gentamycin and 0.25% Trypsin-EDTA were purchased from Lonza (Belgium).

### 1.2. Cell line Propagation:

The cells were grown on RPMI-1640 medium supplemented with 10% inactivated fetal calf serum and 50  $\mu g/ml$  gentamycin. The cells were maintained at 37°C in a humidified atmosphere with 5% CO<sub>2</sub> and were subcultured two to three times a week.

### 1.3. Cytotoxicity evaluation using MTT assay:

For antitumor assays, the tumor cell lines were suspended in medium at concentration  $5 \times 10^4$  cell/well in Corning® 96-well tissue culture plates, and then incubated for 24 hr. The  $ZnSO_4$  concentrations were then added into 96-well plates (three replicates). 0.5 % DMSO was run for each 96 well plate as a control. After incubating for 24 h, the numbers of viable cells were determined by the MTT test. Briefly, the media was removed from the 96 well plates and replaced with 100  $\mu l$  of fresh culture RPMI 1640 medium without phenol red then 10  $\mu l$  of the 12 mM MTT stock solution (5 mg of MTT in 1 mL of PBS) to each well including the untreated controls. The 96 well plates were then incubated at 37°C and 5% CO<sub>2</sub> for 4 hours. An 85  $\mu l$  aliquot of the media was removed from the wells, and 50  $\mu l$  of DMSO was added to each well and mixed thoroughly with the pipette and incubated at 37°C for 10 min. Then, the optical density was measured at 590 nm with the micro plate reader (Sun Rise, TECAN, Inc, USA) to determine the number of viable cells and the percentage of viability was calculated as  $[(OD_t/OD_c)] \times 100$  where **OD<sub>t</sub>** is the mean optical density of wells treated with the tested sample **OD<sub>c</sub>** is the mean optical density of untreated cells

The relation between surviving cells and  $ZnSO_4$  concentrations is plotted to get the survival curve of each tumor cell line after treatment with the specified compound. The 50% inhibitory concentration (IC<sub>50</sub>), the concentration required to cause toxic effects in 50% of intact cells, was estimated from graphic plots of the dose response curve for each conc. using Graph pad Prism software (San Diego, CA. USA) (**Rashad et al., 2022**).

## 2. Flow cytometry

### 2.1. Cell cycle analysis by PI assay using flow cytometry

The cells were digested with warm Trypsin-EDTA + warm Phosphate Buffered Saline

(PBS) -Ethylene diamine tetra acetate (EDTA) (0.25%) (500µl + 500µl) with incubation for 10 minutes at 37°C. The mixture was centrifuged 450 rpm for 5 min, and then supernatant was carefully removed. The mixture was washed twice in warm PBS and the cell pellet was re-suspended in 500 µl warm PBS, centrifuged and supernatant was removed. A volume of 150 µl PBS + 350 µl ice-cold 70% ethanol was added and incubated at 4°C for 1 hour to fix the cells. To remove ethanol, the mixture was centrifuged at 350 rpm for 10 minutes and then the supernatant was carefully removed. The mixture was washed twice in warm PBS and the cells were re-suspended in 500 µl warm PBS, then centrifuged and the supernatant was removed. The cells were re-suspended in 100 µl PBS and stored at 4°C for up to 4 days in darkness. The cells were stained with 100 µl of PI (Propidium Iodide) solution + 50 µl RNase A solution (100 µg/ml), and incubated in darkness for 30-60 min (Rashad *et al.*, 2022). The stained cells were read in Attune flow cytometry (Applied Bio-system, USA).

## 2.2. Apoptosis analysis by Annexin V-FITC Assay using flow cytometry

Collect  $1-5 \times 10^5$  cells by centrifugation and supernatant was removed. Cells were then collected, washed twice with warm PBS buffer and the cells were re-suspended 500 µl of 1X Binding Buffer. Add 5µl of Annexin V-FITC and 5µl of propidium iodide (PI 50 mg/ml) and then incubate at room temperature for 5 min in the dark (Vermes *et al.*, 1995). Analyze Annexin V-FITC binding by flow cytometry (Applied Bio-system, USA).

## 3. Quantitative RT-PCR analysis

Total RNA was isolated from rat liver using GeneJET RNA Purification Kit (Thermo Scientific, # K0731, USA) according to the manufacturer's protocol. Total RNA (5µg) was reverse transcribed using Revert Aid H Minus Reverse Transcriptase (Thermo Scientific, #EP0451, USA) to produce cDNA as previously described (Rashad *et al.*, 2018). The cDNA was used as a template to determine the relative expression of the apoptosis-related genes using Step One Plus real time PCR system (Applied Bio system, USA). The primers were designed by Primer 5.0 software. Forward and reverse primer sequences for Casp3, Bcl-2, p53 and GAPDH inflowing table (1).

**Table (1):** Forward and reverse primer sequences for and *Casp3* genes.

Gene	Forward primer(5' ----- 3')	Reverse primer(3' ----- 5')
Casp3	TTCATTATTCAGGCCTGCCGAGG	TTCTGACAGGCCATGTCATCCTC
Bcl-2	CATGCAAGAGGGAAACACCAGA	GTGCTTTGCATTCTTGATGAGGG
p53	AGAGTCTATAGG CCACCCC	GCTCGACGCTAGGATCTG AC
GAPDH	TGCACCACCAACTGCTTAGC	GGCATGGACTGTGGTCATGAG

The housekeeping gene GAPDH was used as a reference to calculate fold change in target gene expression. A 25µL PCR mix was prepared by adding 12.5 µL of 2X Maxima SYBR Green/ROX qPCR MM (Thermo Scientific, # K0221, USA), 2 µL of cDNA template, 1 µL forward primer, 1 µL reverse primer, and 8.5 µL of nuclease free water. The thermal cycling conditions were as follows: initial denaturation at 95°C for 10 min, 40-45 cycles of amplification of DNA denaturation at 95°C for 15 s, annealing at 60°C for 30 s, extension at 72°C for 30 s. At the end of the last cycle, the temperature was increased from 63 to 95°C for melting curve analysis. The cycle threshold (Ct) values were calculated for target genes and the housekeeping gene, and relative gene expression was determined using  $2^{-\Delta\Delta Ct}$  method (Livak and Schmittgen, 2001).

## 4. Yeast Comet assay (YCA)

The in vitro Comet assay was performed using the first procedure published by (Rashad *et al.*, 2021). We used yeast culture media with the concentrations of ZnSO<sub>4</sub> (50, 75, 100 µg/ml). A medium without chemical components was also employed as an untreated control. 1 g of cell pellets was placed in a one-cubic-centimetre container with cold PBS.

This suspension was filtered after five minutes of stirring. 100 µl of cell suspension was combined with 600 µl of low-melting agarose (0.8 percent in PBS). On pre-coated slides, one hundred percent of this mixture was spread out. For fifteen minutes, the coated slides were immersed in lyses buffer (0.045 M TBE, pH 8.4, containing a pair of 0.5% SDS). The slides were placed in an activity chamber with a same TBE buffer but no SDS. The coated slides were placed in the electrophoresis tank filled with electrophoresis buffer at 4 °C and an electric field of

2 V/cm for 15 min. neutralize the micro gels by neutralization buffer at room temperature for 10 min. drain neutralization buffer and samples in ethanol 76 % and subsequently in 96 % both for 10 min at room temperature. Each slide stained by 50  $\mu$ L of ethidium bromide (20 mg/ml) staining. The polymer fragment migration patterns of one hundred cells for each exposure level were analyzed with a visible radiation magnifier while the samples were still moist (With excitation filter 420-490nm [issue 510 nm]). The tail lengths of extraterrestrial objects were measured from the nucleus to the top of the tail with a 40x increase to count and measure the comet's size. Observations of Gel Red-stained polymer were done using a 40x objective on a fluorescence magnifier to visualize polymer damage. By measuring the length of polymer migration and the proportion of migrated polymer, an extraterrestrial object five image analysis code developed by Kinetic Imaging, Ltd. (Liverpool, UK) connected to a CCD camera was used to assess the quantitative and qualitative extent of polymer injury within the cells. The program then estimated the tail moment. In most cases, fifty to one hundred randomly selected cells were evaluated per sample according to (Rashad *et al.*, 2021).

### 5.1. knockout yeast strains of choice

haploid knockout strains with completely distinct genotypes were used in this investigation, and the sequences of each strain were chosen and aligned with human sequence information in NCBI (The National Center for Biotechnology Information). Four genes aligned with cancer-related human genes were chosen to correspond with the yeast genes used in this investigation (Table 2).

**Table (2):** Selected yeast proteins which matched with cancer related human genes.

Selected strains	Selected genes of yeast strains (genotypes)	Homologous genes in human
YMR177W	MMT1	SLC30A9
YMR199W	CLN1	CCNA1
YMR224C	MRE11	MRE11
YMR243C	ZRC1	SLC30A10

### 5.2. Selection of yeast haploid strains deficient in genes similar to human cancer genes

The genotypes of yeast haploid (knockout) strains were chosen based on (Clustal Omega Multiple

Sequence Alignment EMBL-EBI) alignment between human and yeast sequence similarity Table (2).

### 5.3. Protein-protein interaction prediction

In accordance with the sequence, the interaction network was used. GENEMANIA (<http://www.genemania.org>) is a flexible, user-friendly web interface for evaluating gene function hypotheses, examining sequence lists, and prioritizing genes for specific experiments.

### Sources of information

Co-expression information from the organic phenomenon Omnibus (GEO); physical and genetic interaction information from Bio GRID; foretold macromolecule interaction information supported by orthology from I2D; and pathway and molecular interaction information from Pathway Commons, which includes data from Bio GRID, Memoria, and Pathway Commons. Yeast protein-protein interaction network, Human protein-protein interaction network

### 6. Statistical analysis

All the data were expressed as means  $\pm$ S.E. The statistical significance was evaluated by one-way analysis of variance (ANOVA using SPSS, 18.0 software, 2011 and the individual comparisons were obtained by Duncan's multiple range test (DMRT). Values were considered statistically significant when  $p < 0.05$ .

## Results

### 1. Cytotoxic effect by MTT assay

Zinc Sulphate revealed its cytotoxic activity at the different concentrations on the proliferation of HepG2, A549 and Wi38 cells in comparison to a positive control were determined using the MTT cytotoxic assay.

In general, the cell viability was decreased gradually as the concentrations of zinc Sulphate increased as illustrated in Table (3). The cytotoxicity and cell viability of zinc Sulphate. The viability of positive control was reduced as the concentration increased of tested zinc Sulphate. The Dose inducing 50% cell growth inhibition (IC50) against hepatoma cell line cells (HepG2) is presented in Table (3) and Dose-response curves for cell viability in Figure (1).

**Table (3).** Effect of different ZnSo<sub>4</sub> concentrations on hepatocellular carcinoma cells (HepG2)

ZnSo <sub>4</sub> conc. ( $\mu$ g/ml)	Viability %	Inhibitory %	S.D. ( $\pm$ )
---------------------------------------	-------------	--------------	----------------

ZnSO <sub>4</sub> conc. (µg/ml)	Viability %	Inhibitory %	S.D. <sup>11</sup> (±)
500	26.49	73.51	3.75
250	57.08	42.92	3.14
125	81.43	18.57	1.79
62.5	98.12	1.88	0.46
31.25	100	0	
15.6	100	0	
7.8	100	0	
3.9	100	0	
2	100	0	
1	100	0	
0	100	0	

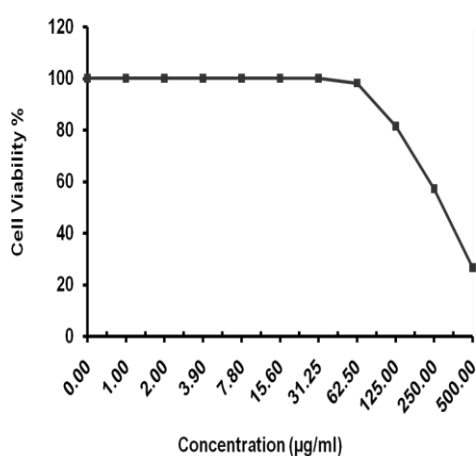


**Fig. 1:** Inhibitory activity of ZnSO<sub>4</sub> concentrations against Hepatocellular carcinoma cells (**HepG2**)

The cell viability was decreased gradually as the concentrations of zinc Sulphate increased as illustrated in Table (4). The cytotoxicity and cell viability of zinc Sulphate. The viability of positive control was reduced as the concentration increased of tested zinc Sulphate. The Dose inducing 50% cell growth inhibition (IC<sub>50</sub>) against lung cell line cells (**A549**) is presented in Table (4) and Dose-response curves for cell viability in Figure (2).

**Table (4).** Effect of different ZnSO<sub>4</sub> concentrations on lung carcinoma cells (**A549**)

ZnSO <sub>4</sub> conc. (µg/ml)	Viability %	Inhibitory %	S.D. <sup>11</sup> (±)
500	34.68	65.32	2.34
250	78.94	21.06	2.82
125	94.03	5.97	1.75
62.5	99.26	0.74	0.48
31.25	100	0	
15.6	100	0	
7.8	100	0	
3.9	100	0	
2	100	0	
1	100	0	
0	100	0	

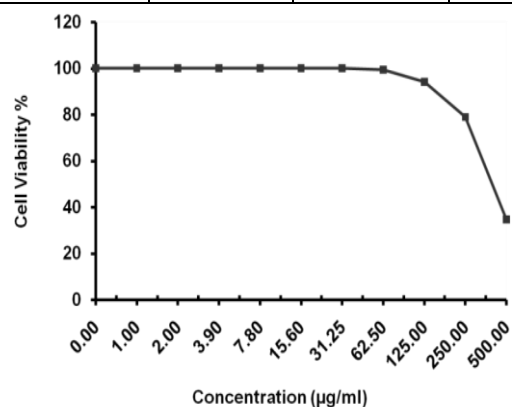


**Fig. 2:** Inhibitory activity of ZnSO<sub>4</sub> concentrations against lung carcinoma cells (**A549**)

The cell viability was decreased gradually as the concentrations of zinc Sulphate increased as illustrated in Table (5). The cytotoxicity and cell viability of zinc Sulphate. The viability of positive control was reduced as the concentration increased of tested zinc Sulphate. The Dose inducing 50% cell growth inhibition (IC<sub>50</sub>) against normal lung cell (**Wi38**) is presented in Table (5) and Dose-response curves for cell viability in Figure (3).

This results according to (**Rashad et al., 2019**) four different types of human cell lines; namely, colon carcinoma (Caco-3), breast carcinoma (MCF7), lung carcinoma (A549) and normal lung cell line (Wi38) were treated. Viability in shapes of the cells showed considerable variations between control and treatment and confirmed the carcinogenic effect of these components.

**Table (5).** Effect of different ZnSO<sub>4</sub> concentration on human lung fibroblast normal cells (**Wi38**)

ZnSO <sub>4</sub> conc. (µg/ml)	Viability %	Inhibitory %	S.D. (±)
500	<b>43.87</b>	<b>56.13</b>	<b>3.69</b>
250	<b>85.06</b>	<b>14.94</b>	<b>2.81</b>
125	<b>97.31</b>	<b>2.69</b>	<b>0.75</b>
62.5	<b>100</b>	<b>0</b>	
31.25	<b>100</b>	<b>0</b>	
15.6	<b>100</b>	<b>0</b>	
7.8	<b>100</b>	<b>0</b>	
3.9	<b>100</b>	<b>0</b>	
2	<b>100</b>	<b>0</b>	
1	<b>100</b>	<b>0</b>	
0	<b>100</b>	<b>0</b>	

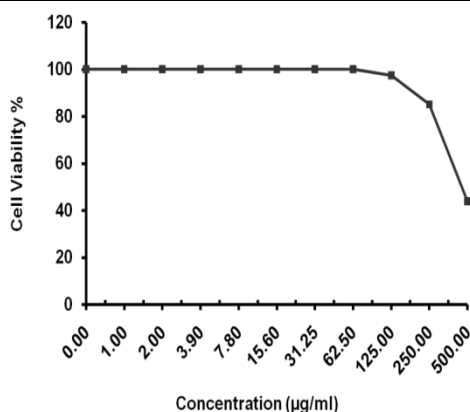


**Fig. 3:** Inhibitory activity of ZnSO<sub>4</sub> concentrations against human lung fibroblast normal cells (Wi-38)

### 2.1. Cell cycle analysis by PI assay using flow cytometry

ZnSO<sub>4</sub> at concentrations 75µg/ml affected the DNA content of HepG2 cells. The G0/G1 phase showed a decrease from 44.69% to 42.51% for control. Similarly, the S phase percentage also exhibited a decrease from 39.54% to 35.31% in the control and ZnSO<sub>4</sub>. In the G2/M phase there was an increase in the DNA contents of the HepG2 cells when treated with ZnSO<sub>4</sub> (23.43%) comparing with the control (15.77%) as illustrated in **Table (6)**. These results showed significant accumulation of HepG2 cells in the G2/M phase, and confirmed that ZnSO<sub>4</sub>

has marked cytotoxic effect via induction of G2/M phase arrest of the cell cycle as shown in **Figure (4)**.

**Table (6):** Average % of DNA content in each cell cycle phase using HepG2 cells treatment

Groups	Percentages of DNA content each in cell cycle phase			
	G0/G1 phase	S phase	G2/M phase	Pre-G1
HepG2-control	44.69	39.54	15.77	1.64
HepG2-treated with ZnSO <sub>4</sub>	41.26	35.31	23.43	8.92

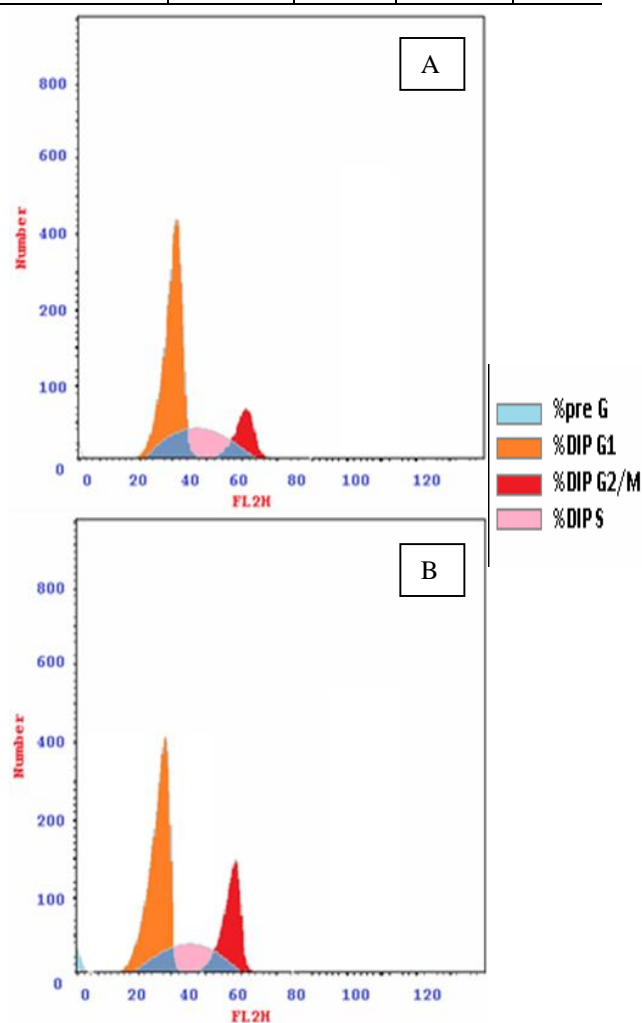


**Fig. 4:** (A) liver cancer cell line (HepG2) - untreated (B) Liver cancer cell line (HepG2) where treated with ZnSO<sub>4</sub> at concentration 75µg/ml and effect at G2/M cell cycle arrest.

### 2.2. Apoptosis analysis by Annexin V-FITC Assay using flow cytometry

Apoptosis is a tightly regulated process under the control of several signaling pathways, such as the mitochondrial pathway and caspase cascade. Effects of ZnSO<sub>4</sub> on HepG2 cells at the 75µg/ml concentration was applied to the cell culture to determine cell necrosis and apoptosis. Apoptosis and necrosis were measured with Annexin V-FITC/PI double-labeled flow cytometry (Figure 5). The apoptotic rate was calculated as the percentage of the early and late apoptotic cells. As shown in (Table 7), change in the apoptotic rate was observed in ZnSO<sub>4</sub>-treated HepG2 cells, as they were 0.84% and 1.83% for early and late apoptotic cells, respectively. While, control were 0.43% and 0.15% for early and late apoptotic cells, respectively. The necrotic effect was 6.25% for ZnSO<sub>4</sub>-treated HepG2 cells and 1.06% for control. These results showed ZnSO<sub>4</sub> had significant impact of apoptotic and necrotic effect on HepG2 cells.

**Table (7).** Apoptotic and necrotic effect on **HepG2** when treated with ZnSO<sub>4</sub>

Groups	Percentage of apoptosis		Percentage of necrosis
	early	late	
HepG2-control	0.43	0.15	1.06
HepG2-treated with ZnSO <sub>4</sub>	0.84	1.83	6.25

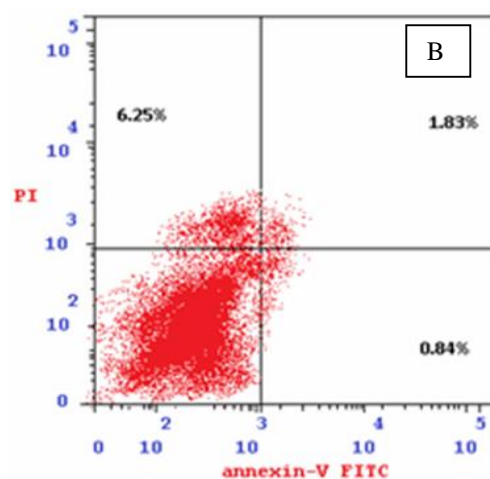
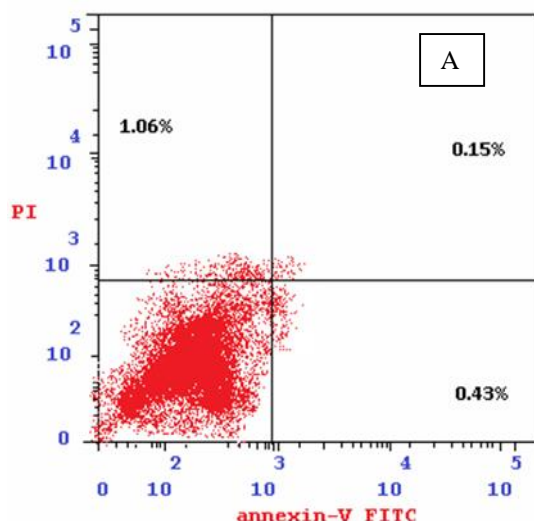


**Fig. 5:** (A) liver cancer cell line (HepG2) – (B) untreated liver cancer cell line (HepG2) where treated with ZnSO<sub>4</sub> at concentration 75µg/ml. Nt .Lower left (live cells) - lower right (early apoptosis) - upper left (necrotic cells) - upper right (late apoptosis)

#### 4. Quantitative RT-PCR analysis

##### ZnSO<sub>4</sub> induced genotoxicity of some related genes, *casp3*, *Bcl-2* and *p53* in HepG2 cells

The role of apoptosis in ZnSO<sub>4</sub> induced cytotoxicity on liver cancer cell lines (HepG2) was studied. The expression levels of apoptosis-related genes such as *casp3*, *p53* and *Bcl-2* in HepG2 cells were estimated by real time PCR (qRT-PCR). *Casp3* increased by 3.12285797 than control (Table 8), also *p53* increased by 2.577512 than normal (Table 8). *Bcl-2* decreased by 0.6682521 than control (Table 9), showed that, compared to the untreated group control (Table 10), the expression levels of *casp3* gene and *p53* gene were increased, whereas that of *Bcl-2* gene was decreased (Figure 6). These results indicated that the ZnSO<sub>4</sub> killed HepG2 cells through apoptosis mechanism mainly via over expression of *casp3* and *p53* genes, while *Bcl-2* down regulated.

**Table (8):** Effect of ZnSO<sub>4</sub> compound administration on the relative expression of *casp3* gene in HepG3 cells.

Groups	Casp3 Ct values	Δ Ct	ΔΔ Ct	Relative quantification
Control HepG2	33.88	10.2	0.00	1.00
Treated HepG2	31.32	8.39	-1.78	3.122857

**Table (9):** Effect of ZnSO<sub>4</sub> compound administration on the relative expression of *p53* gene in HepG3 cells.

Groups	<i>p53</i> Ct values	Δ Ct	ΔΔ Ct	Relative quantification
Untreated HepG2	33.08	9.37	0.00	1.00
Treated HepG2	30.82	7.89	-1.48	2.577512

**Table (10):** Effect of ZnSO<sub>4</sub> compound administration on the relative expression of *Bcl-2* gene in HepG2 cells.

Groups	<i>Bcl2</i> Ct values	Δ Ct	ΔΔ Ct	Relative quantification
Untreated HepG2	28.51	4.8	0.00	1.00
Treated HepG2	28.36	5.43	0.36	0.6682521

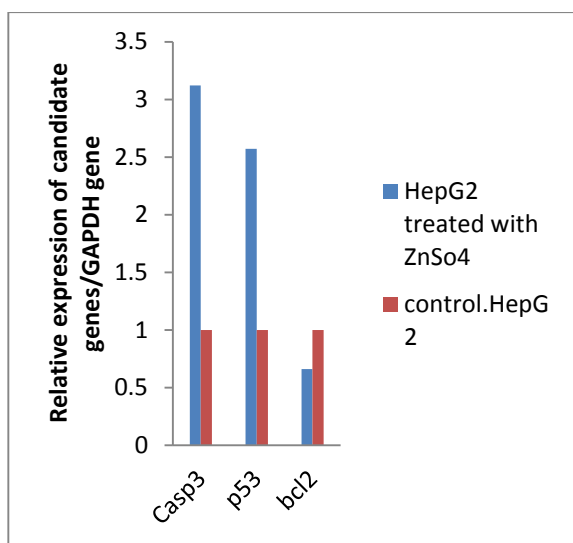


**Fig. 6:** Effects of ZnSO<sub>4</sub> on apoptosis-related genes after exposure to 75μg/ml, mRNA expression of *casp3*, *Bcl-2* and *p53* was assessed by quantitative RT-PCR \*P < 0.05, compared to the control group

### 5. Toxicity to (YKO) strains tested with Zink sulphate by comet assay

Zink sulphate displayed varying degrees of yeast significant genotoxic effects on YKO in accordance with the comet assay. The concentrations of ZnSO<sub>4</sub> are (50, 75, 100 μg/ml) revealed its genotoxic effect.

Control	concentration of ZnSO <sub>4</sub> (50μg/ml)	concentration of ZnSO <sub>4</sub> (75 μg/ml)	concentration of ZnSO <sub>4</sub> (100 μg/ml)
---------	--	---	--

The genotoxic effects of the MMT1, CLN1, MRE11 and ZRC1 genes were severe, whereas the genotoxicity of the MMT1 gene was low than other genes. The distribution of the share of determined comets for Zinc sulphate was shown in **Table (11)**. It should be noticed that the yeast predicted significantly more comets than the control for each of the four tested genes (**Fig. 7**), indicating that the tested ZnSO<sub>4</sub> caused a large number of identified deoxyribonucleic acid damages. The cells were clear that Zinc sulphate treatment caused significant damage to each of the four genes evaluated.

**Table (11):** Image analysis of comet assay parameters in cells of all groups after ZnSO<sub>4</sub> treatment.

Concentrations	Tail Length (px)	Tail DNA (%)	Tail Moment	Tail Olive Moment
<b>Control MMT1 (A)</b>	3.2	16.42885	0.856675	1.331495
50 μg/ml (A1)	5.84	18.56993	2.698397	2.569634
75 μg/ml (A2)	7.96	24.76888	3.678652	3.649392
100 μg/ml (A3)	10.9	26.52228	5.214025	4.659043
<b>Control CLN1 (B)</b>	4.14	17.84848	1.408786	2.093441
50 μg/ml (B1)	7.02	21.30251	2.494028	3.093563
75 μg/ml (B2)	9.7	30.84848	3.890823	4.417296
100 μg/ml (B3)	15.86275	38.18079	8.828677	6.79219
<b>Control MRE11 (C)</b>	3.7	11.32471	0.644259	1.424435
50 μg/ml (C1)	5.74	18.33586	1.895839	2.269366
75 μg/ml (C2)	9.66	26.86337	4.662948	4.175398
100 μg/ml (C3)	17.48	30.11288	9.030276	6.586223
<b>Control ZRC1 (D)</b>	4.510204	15.1704	0.988069	1.662803
50 μg/ml (D1)	7.627451	23.06511	3.322405	4.314785
75 μg/ml (D2)	12.08	25.41651	6.076189	5.287539
100 μg/ml (D3)	18.66	38.52412	10.73177	8.686483

Different superscript letters in the same column of tail length showed significance difference at P < 0.05.

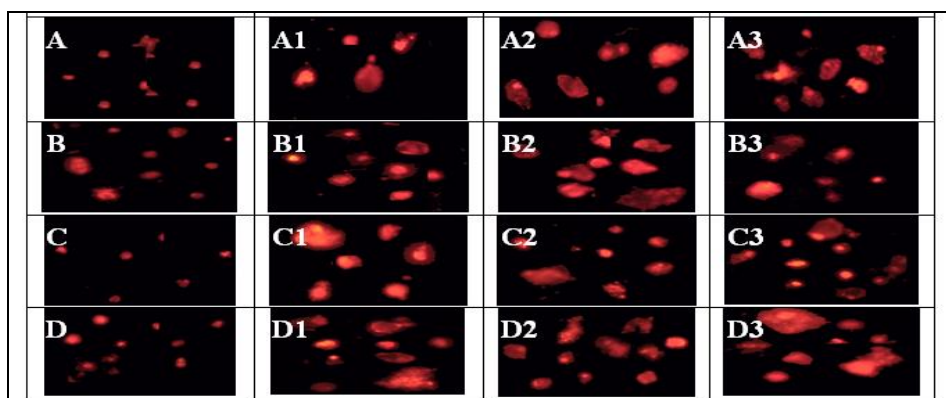


**Fig. 7:** Photomicrographs showing DNA damage in yeast strains using the Comet assay and Zink sulphate at a dose of (50, 75, 100 µg/ml). Control cells A: control MMT1 gene; A1, A2, A3: treated MMT1 gene; B: control CLN1 gene; B1, B2, B3: treated CLN1 gene; C: control MRE11 gene; C1, C2, C3: treated MRE11 gene; D: control ZRC1gene; D1, D2, D3: treated ZRC1 gene.

**3.4. Selection of yeast haploid strains devoid of genes similar to specific human cancer genes in vitro.**

Genotypes of yeast haploid (knockout) strains were determined based on sequence similarity results between human and yeast sequences. Figure (8)

depicted the results of an alignment between the human SLC30A9 and the yeast MMT1sequences. MMT1 Putative metal transporter involved in mitochondrial iron accumulation; MMT1 has a paralog, MMT2 that arose from the whole genome duplication.

NC_001145.3:MMT1	-----AAATTGAAAAGGCTGCAATAA	208
NC_000004.12:SLC30A9	CTGTCTCAAAAAAAAAAAAAAAAAAGAAAAAGAAAAAGGTGGAGGAAAAAGTGCCTGCAGAGG	50319
NC_001145.3:MMT1	AG-----GAAATTGGAGAA--AAATCCTC-----AATACCAAAAA	240
NC_000004.12:SLC30A9	AGATTGAGGGAGGAGTAAGGGAGAAAAGTAGAAAAGAAAAACGAGGAGTGTATTAGTCCATTTT	50379
NC_001145.3:MMT1	TTAGCTGAAGC-----ATTCAACAGTCATGATCATGTTCAATT-----TA	279
NC_000004.12:SLC30A9	CACGCTGCTGATAAAGACATACCCAAAGACTGGGCAATTTACAAAAGAAAGAGGTTTAATT	50439
NC_001145.3:MMT1	CGTGAATCAGAGACCGAGCAAAA-----CGACATAAATTTCAATTG-----G-----GC	321
NC_000004.12:SLC30A9	GGACTTACAGTTCCTGGTGGCTAGGGAAAGCCTCACAATCATGGTGGAAAGGCAAGGAGGAGC	50499
NC_001145.3:MMT1	ACGATACGAGACTACA-----A-----AAGCAGTAAATGTGAGCAA--GCTGATAAGCCTTCG	372
NC_000004.12:SLC30A9	AAGTTA--TGTCTTACATGGATGGCAGCAGGCAAAATAGAGCTTGTGCAGGGTAACTCCCA	50557
NC_001145.3:MMT1	TCGTT--GAATCTG-----C--ATTTCGCATACACATTCTCATGGAC-----AT	411
NC_000004.12:SLC30A9	TTTTTAAAAACCATCATCATCTCATGAGCTCATTCACTATCAAAAGAACCAACATGGGAAAG	50617
NC_001145.3:MMT1	ACGCATTCTCATGCTGCTCACA-----ATCCATTATTAGTACTTAGT--A	454
NC_000004.12:SLC30A9	ACCCACCTCATGCTTCAAGTCACTCTCCCACTGCGTCCCTCCCAAAACATGTGGGAATTA	50677
NC_001145.3:MMT1	CTGAGCAAATT--AGGAAAAATGCAGGCG-----TAAGAATCATGSGGTCGG--	500
NC_000004.12:SLC30A9	AGGAGCTACAAGATGAGATTTTGTGGGAGACACAGAGCCAAACCATATCAAGGAGTGTCA	50737
NC_001145.3:MMT1	-----CTTAGGTGTAAACGTTGGTATTGCTATAGGTAATTTTTTGGAGGTATCGTAT	553
NC_000004.12:SLC30A9	AGAAAGCCAAAGGGAAGAGCGTTTGTIT--TTTTT--TTGTGAGACGGAAAT	50784
NC_001145.3:MMT1	TTCA----TTCACAAAGCATTGTTGCGG--ATGCTATCCACGCAATAAAGTGA-----	599
NC_000004.12:SLC30A9	CTCACTCTGTGCCAGGCTGGAGTGCAGTGGTGAATCTCGGCTCACTGCAACCTCCGCC	50844
NC_001145.3:MMT1	--CATGGTTCTGA-----CTTGTGACTTTGCTTTCGGTAGGGCTAGCAGCCAACAAGCC	653
NC_000004.12:SLC30A9	TCCAGGTTCAAGCGATTCTCCTTGCCTCAGCCTCCTGAGTAGCTGG--GACTACAGGCA	50902
NC_001145.3:MMT1	AACCGCTGATTATCCATATGGGTATGGCAAAAATTGAAACTGTTGGTTCCTTGGCAGTTTC	713
NC_000004.12:SLC30A9	CACAT--GT-----TTTAAGGAAATAGCAGGCGCTGGTACAGGCACACACCTGG--AATCTC	50954
NC_001145.3:MMT1	AACAATAT---TAGCCATGGCTGGTATATCAATAGGTTGGAGTTCCTTTTGTGCCTCGT	770
NC_000004.12:SLC30A9	AGCACTTTGGGAGGCTGAGCAGG-----AGGATTACTTGGACTCAGGA	50998
NC_001145.3:MMT1	AGGGCCTGTTATCCCAATACAACTATTGACACCCATAGGAAAACCTAGG-----TCATGCTC	826
NC_000004.12:SLC30A9	ATT-----TCAGA-----CCACCTTGGGCAACATAGTGAGACCTTGTAC	51037
NC_001145.3:MMT1	ATACTTATTC-----TG--AAGACATTATTGAAGACGTTACTGATATCAACGCA	873
NC_000004.12:SLC30A9	CTACAAAAAATTTTTTAAATTAGCTGGGCATGGTGGGTGATG-----TGC--	51083
NC_001145.3:MMT1	GCTGGATTGCCGCCGCTTCCATTGCAGCTAAAGAAT--GGATATTTAGAGCCACAAGAA	931
NC_000004.12:SLC30A9	GCCTGTAG-ACCT---ACTCAGGAACTGAGGCAGGAGAAATCAATTTGAGCCAGGAGT	51137
NC_001145.3:MMT1	A-----GATTGCTA-----TCAACACTAATTCAAATGTACTAATGGCAAA	971
NC_000004.12:SLC30A9	TTAAGGCTACAGTAAAGCTGTGATTATACCACACTGCACCTCCAAAGC-----TGGSCAAAG	51188
NC_001145.3:MMT1	TGCTTGG-----C-----ATC-----ACCG	986
NC_000004.12:SLC30A9	AACAAGACCCCTGTCTTTAAAAAATAAATAGCCAGCTAGGGGGTGGCGGGCAAGATGGCTG	51248

NC_001145.3:MMT1	TGTTGATTCATTAACTTCTCTTGTGCTCTGGTTGCAATCAGTACTGGTTATTTGGTTAA	1046
NC_000004.12:SLC30A9	GATAGGAAACAGATCCT-GT-CTGCAGCTCCCAAGTGAATCCATGCAGAA--GTGGATAA	51304
NC_001145.3:MMT1	T-----ATACAATCATT-----GACACGATTGGTGGTTAATTGTTTCTGGTTAA	1093
NC_000004.12:SLC30A9	CTTCTGCATTTCCAGCTGAGGTACCTGGCTCA-----TCTCATTGGGACTGGTCAGA	51356
NC_001145.3:MMT1	-----TTATCAAGGCTGGTGGCG-----AGGGTATGTGCATCGCAATAAAGGAGT	1138
NC_000004.12:SLC30A9	CAGTGGGTGCAGCCCATGGAGGGTGACCCGAAAGCAGGGTGGGGCATTGCCACCCGGGT	51416
NC_001145.3:MMT1	TAATCGATCAGTCAGTTTCTCGTGATGAT-CCACG-C-TACCTAGAGAT-----AGAAA	1189
NC_000004.12:SLC30A9	AGTGCAGGGGTC-----GGGGAACCTCCCTCCCTAGCCAAAGGGAAGCCATGAGGGA	51468
NC_001145.3:MMT1	CTTTGGTTAAAGATACGTTGAACAAACTGATCTCTAATAAATTCTCAGAAACCCATG	1249
NC_000004.12:SLC30A9	CTGTGCTGTGAGGAACGGTGC--ATTCCAG-CCCAGA---TACTACGCTTT-TCCC-ATG	51520
NC_001145.3:MMT1	GATTGAAA GAAGTACGTTACTGTCCTCAGGACCGAATTTAC--GCGGA--CAT-----	1299
NC_000004.12:SLC30A9	G-----TCTTCACAACCCACAGACCAGGAGATTCCCTCGGGTGCCTACACCG	51567
NC_001145.3:MMT1	--TTAACCTTGGAAAGTTCCTTTACAAAAATGGGGCAATATTTTAGG-TGTTAACGAGTTT	1356
NC_000004.12:SLC30A9	CCAGGGCCTTGGG-TTTCAGACAAAACTG-GGCGGCCATTTGGGCAGACCCAAAGCTA	51625
NC_001145.3:MMT1	GAAATTGTGACACATCATTTACGTAATGTGTTAACCAATGAAGTATCGAATTTGAG-AAG	1415
NC_000004.12:SLC30A9	GCT---AGACTAGTTTT-----TTTTCACTCCAGTGGTGCCTCGAATGCCAGTGA	51675
NC_001145.3:MMT1	ACTGGATATTG--AATACGTGGAA-----GAAAAAAATGGTGAGGAAAAATG-----	1459
NC_000004.12:SLC30A9	ACAGAACCTTTTAAATCCCTTGGAAAGGGGGCTGAAACAGGGAGCTAAGTGGTCTAGCTC	51735
NC_001145.3:MMT1	ACTGGATATTG--AATACGTGGAA-----GAAAAAAATGGTGAGGAAAAATG-----	1459
NC_000004.12:SLC30A9	ACAGAACCTTTTAAATCCCTTGGAAAGGGGGCTGAAACAGGGAGCTAAGTGGTCTAGCTC	51735
NC_001145.3:MMT1	AGCATATC-----	1467
NC_000004.12:SLC30A9	AGCAGATCCACCTCCAGAGAGCCAGAAAGCTAAGATCCACTGGCTTGAATTTCTGGCT	51795
NC_001145.3:MMT1	-----	1467
NC_000004.12:SLC30A9	GCCAGCACAGCTGTCTGAAGTTGACATGGGATGCTTGAAGTTTGGTGTGTGTTGGGAAGT	51855
NC_001145.3:MMT1	-----AAGGGACA-ACAAAACACTAC-----A-----	1486
NC_000004.12:SLC30A9	GGGGTTGGGGACCACTTACTGAGGCTTGAAGTGGCAAGTTTCCCTCACAGTGTAAA	51915
NC_001145.3:MMT1	-----AAGAAGATGTTCTTATTAAGCACGACCATACGAATACTC-----	1525
NC_000004.12:SLC30A9	CAAAGCCATCAGGAAGTTGAACTGGACAGAAACCCACCGT-AGCTCAGCAAAAGCCACTGT	51974
NC_001145.3:MMT1	-----	1525
NC_000004.12:SLC30A9	AGCCAGACTGCCTCTCTAGATTTCTTCTCTCTGGGACAGGCACTCTCTGAAAGAAAGGCC	52034
NC_001145.3:MMT1	-----	1525
NC_000004.12:SLC30A9	AGCAGTCCCGGTCAAGGGGCTTATAGATAAAACCTCTCATCTCTCTGGGACAGAAAACCTGG	52094
NC_001145.3:MMT1	-----	1525
NC_000004.12:SLC30A9	GGGTAGGGGCGGCTGTGGGCGAGCTTACGACAGACTTAAACGTTCTCTGCTGCTGGCTCT	52154
NC_001145.3:MMT1	-----	1525
NC_000004.12:SLC30A9	GAAAGAGAGCAGCGGATCTCCACGACAGCGCTCGAGGTCTGCTAAGGGACAGACTGCCCTC	52214
NC_001145.3:MMT1	-----	1525
NC_000004.12:SLC30A9	CTCAAGTGGGTCCTTGAACCCCATGCCTCTGATGGGAGATACCTCCAGCAGGGATCA	52274

**Fig. 8:** Gene alignment between human gene SLC30A9 and the yeast MMT1 in the Clustal Omega web site ('\*' indicates identical between two aligned, '-' indicates gaps missing of one) and ('.' indicates low similarity, ':' indicates more similarity used to denote the level of similarity that are not identical) at position.

Figure (9) depicted the results of an alignment between the human CCNA1 and yeast CLN1 sequences. G1 cycle is involved in regulation of the cell cycle; activates Cdc28p kinase to promote the G1 to S phase transition; late G1 specific expression depends on transcription factor complexes, MBF

(Swi6p-Mbp1p) and SBF (Swi6p-Swi4p); CLN1 has a paralog, CLN2, that arose from the whole genome duplication; cell cycle arrest phenotype of the *cln1 cln2 cln3* triple null mutant is complemented by any of human cyclins CCNA1, CCNA2, CCNB1, CCNC, CCND1 or CCNE1.



NC_001145.3	CT---TCTCCAAGCACATATTCTTCGGGAAACCAATTAT-----ACTCCA-----	1269
NC_060937.1	CCTCCTCCTTCATGCCCCAGTCTCAGCTGATCACTTTGTATCTTATTTTTCTAAAAATATA	2766
NC_001145.3	-----ATGCGAAACTTC-----AG--TGAC--AATCAGACAACAGTGT	1304
NC_060937.1	GAAGCAAGCAGAAAGAGAATCTCCACATGTCCCTGTGTGCCATATAATCTGCCATCTACAT	2826
NC_001145.3	TTTCAGT--ACTACCAACATTGACCATTCA----TCGCCGATCACC-----CCTCAC-A	1351
NC_060937.1	--CCTGTTATGTGACTGCTATGTCCCTGTGTCATGCGAGGTGCCCCCCCCCCCGCCA	2884
NC_001145.3	T--GTACA-----CTTTTAAATCAG-TTTAAAAACGAA-----	1380
NC_060937.1	TGCGTACAATATACTCGTGTCTTTGCTTCTTCAAGGATGTTACTCTAGCCACTTTTCT	2944
NC_001145.3	-----AGTG--C--TTGTGACAGTGCCATAAGCGTAAGCAGTCTA-----	1416
NC_060937.1	TTCTCTCATGATTTTTTTTCTTCTACTGGGCCAAATCTGTAAGCATACAAATATTGCG	3004
NC_001145.3	-----	1416
NC_060937.1	CATTTTCCCATCTTAAAAACCTTTCAACTAAACGCTCCCTCTGAGTATTACAAACCTGGA	3064
NC_001145.3	-----CCTAATCAAACCC-----	1429
NC_060937.1	ATCTGGACCACAGGGAAGAGTTGACTTTGTAAAATCACCTTGACCGGTCCCTTTTTCAG	3124
NC_001145.3	---AAAATGGTAA-----ATGCCATTATCAAGCAATTA-----	1460
NC_060937.1	CTAGAAATGGTGACGAATTTTCTTTGTTAGTTTTCCAAATATCAAGGAAATAGGTCTAGGA	3184
NC_001145.3	-----TCAGA-----ATATGATGCTAGAAGAAAAGAA--TAAA--GA	1493
NC_060937.1	GCTGTTTGCAATTATGTCGATTAAAGTAATTTAAAGTGCCTTAAAGAAAATTAAGTAAATGGGA	3244
NC_001145.3	GAATAGAATTCCCAA-----	1508
NC_060937.1	CAGAAAGCTATCCCATTTAAAGCCACATATCTTGAGAGTTTGTGCTATCTTGACATATATA	3304

**Fig. 9:** Gene alignment between human gene CCNA1 and yeast CLN1 gene in the Clustal Omega web site ('\*' indicates identical between two aligned, '-' indicates gaps missing of one) and ('.' indicates low similarity, ':' indicates more similarity used to denote the level of similarity that are not identical) at position.

Figure (10) shows the results of alignment between human and yeast MRE11 sequences. Nuclease subunit of the MRX complex with Rad50p and Xrs2p; complex functions in repair of DNA double-strand breaks and in telomere stability; Mre11p

associates with Ser/Thr-rich ORFs in premeiotic phase; nuclease activity required for MRX function; widely conserved; forms nuclear foci upon DNA replication stress.

NC_001145.3:c720653-718575	-----ATGGACTATCCTGATCCAGACACAATAAGGATTTTAACTACTACAGATAA	50
NC_000011.10:c94512412-94415570	TTGTTCCCTTAACTGCAAGTAAAGTCGAGTATAGTCAACTGGCCTGTTTCTGGGTGCTT	88080
NC_001145.3:c720653-718575	TCATGTGGGTTACAACGAAAAATGATCCCACTACTG-GCGATGATTCTTG---GAAAACTT	106
NC_000011.10:c94512412-94415570	TCA-GAGGGCCACAGCTCTATATAGATCTTTACTGTGCTAGATTCTGCCCCGGGTGTC	88139
NC_001145.3:c720653-718575	TCCATGAAGTCATGATGTGCGCAAAAAATAACAACGTAGACATGTTGTACAGTCCGGTG	166
NC_000011.10:c94512412-94415570	ACAGAGATGTATATTGGCAGAAATTTTGGTGTGTAAATTTGGCTGT--GATCCAGTA	88197
NC_001145.3:c720653-718575	ATCTTTTTCACGTGAATAAGCCTTCCAAAGAGTCACTCTACCAAGTACTGAAGAC-TTTG	225
NC_000011.10:c94512412-94415570	GCTGGCATTAAACATTAGTGTCCAGTGGATAGGCTCTTACTAGCTGCATAGTTCTTTTG	88257
NC_001145.3:c720653-718575	AGATTATGTTGCATGGGTGACAAGCCTTGCAGTTAGAATTATTGAGCGAT-CCCTCACA	284
NC_000011.10:c94512412-94415570	TATTTCTGTGTGTTACAGCCGTGCTGTGGTGGGGTTGGGGAGAGAGATGACCACTCA	88317
NC_001145.3:c720653-718575	AGTTTTTCACTACGATGAATTTACCAACGTTAACTATGAGGACCCCCAATTTAATATTTT	344
NC_000011.10:c94512412-94415570	TAAGGGCCACTCC-----TGACCATGG-----GTGAGGTCCCTCCTATCACTGGCAC	88365
NC_001145.3:c720653-718575	TATTCCTGATTCGGCATATCAGGTAATCATGATGATGCGTGGGGGACTCACTGTTGTG	404
NC_000011.10:c94512412-94415570	TGTACCTGCATTACTGTTGTTGGTGTCTTGG-----GTTGACGGGCTCCCTTAGACAGA	88420
NC_001145.3:c720653-718575	TCCTATGGATATACTTTCATGCGACTGGTCTAATAAATCATTTTC-GGGAAAGTCATCGAAT	463
NC_000011.10:c94512412-94415570	GGCCATGGCTGCCAGACAGGCCACACCCCTTCCAGACCAGCACTGTGGAGGAAAGGCATGT	88480
NC_001145.3:c720653-718575	CTGATAAAATAAAAGTGTGCGCAATATTTTTCAGAAAGGGTCCACTAAGTTAGCATTGT	523
NC_000011.10:c94512412-94415570	CCCATTCTGCACTGGC---CCACGAACCCAGTGTCTCACTCCTTTCAAGTGTCTGAAA	88537









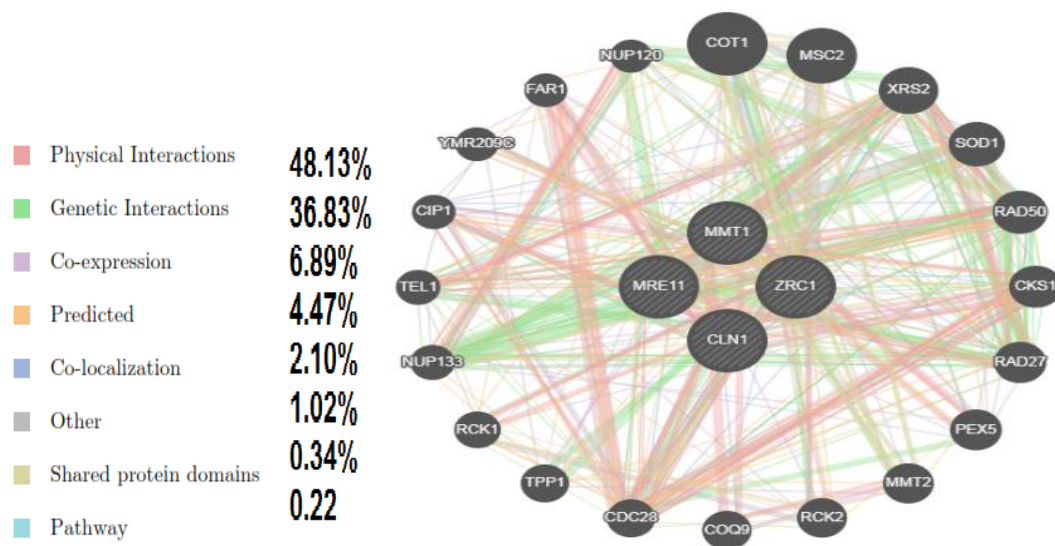


**Fig. 12:** The yeast cell-cycle default query with all default parameters. The yeast cell-cycle default query with all default parameters. Using the default network weighting approach, the yeast cell-cycle default query.

Four yeast inquiries are being displayed by Gene MANIA (Fig. 13). The networks that result are completely distinct, with various totally different absolutely different relationships and four separate relevant genes in yeast that are linked by a pathway to the query list. Physical interaction (48.13%), co-expression (6.89%), Predicted (4.47%), co-localization (2.10%), other (1.02%), genetic interaction (36.83%), Shared protein domains (0.34%), Pathway (0.22%) and common macromolecule domains are some of the other levels of question customization (0.59 percent). Gene

MANIA displays the results of gene queries in Effects of Knowledge Set Choice on Topology. Mistreatment of all default parameters in the human default question. Mistreatment default network weight approach, which is a human default question. YKO lacking genes that are similar to cancer genes in humans were chosen. The ability to predict protein-protein interactions in yeast and human could lead to an assessment of the degree of deliberate similarity of some cancer-related genes between the two organisms.

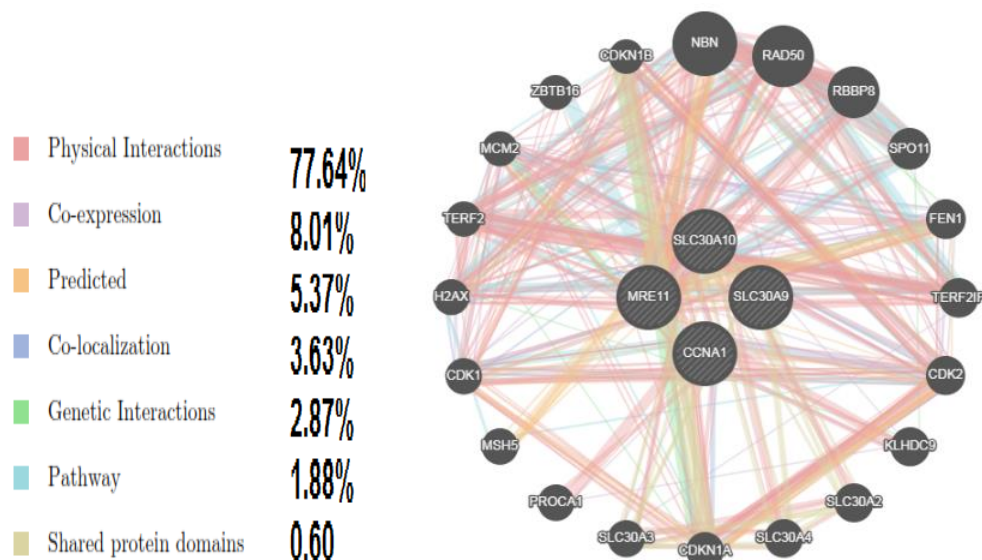


**Fig. 13:** The human default query, using all default parameters. The human default query, using default network weighting method



#### 4. Conclusions

In similar to **Yuan et al (2012)** the cell viability of A549 first increased and then decreased with increasing zinc concentration, the turning point occurring at 50 mM ZnSO<sub>4</sub>. A higher zinc concentration ( $\geq 75$  mM) finally decreased the A549 cell viability. Also **Wang et al (2013)** indicted the cell viability of HepG2 decreased with increasing ZnSO<sub>4</sub> concentration, when treated for 48 h. **Wang et al (2016)** Viability of MDAMB231 cells decreased to ~80 % after being treated with 50  $\mu$ M ZnSO<sub>4</sub> for 24h, The significant increase on intracellular zinc content in ZnSO<sub>4</sub>-treated cells promoted cell death. **Zhao et al (2015)** showed an elevated ZnSO<sub>4</sub> concentrations reduced A549 cell viability, although the viability of A549 cells remained about 50% and 20% after treatment with 500  $\mu$ M ZnSO<sub>4</sub> for 9 and 24 h, respectively. Results in this investigation are in parallel with those obtained by **Cui et al. 2002**. They found that the cell cycle progression of HepG2 cells was readily altered by depressed intracellular zinc status. An elevated percentage of the ZD cells were found to be in G1 phase, and the proportion of S phase cells was markedly reduced by zinc depletion. It was suggested that zinc is critical for the progression of HepG2 cells from G1 to S phase. However, the mechanism of how zinc depletion impairs the G1-to-S phase transition remains unclear.

Consistent with previous studies in HepG2 cells, zinc depletion led to a reduction in DNA content per plate. **Libin et al. 2002** stated that addition of only 0.4 M zinc significantly restored the DNA content per plate, indicating that minimal changes of cellular zinc status have profound influence on cell proliferation and DNA synthesis. On the other hand, the zinc depletion-reduced DNA content in zinc-depleted HepG2 cells may also reflect the possibility that some of these cells were undergoing apoptosis (**Nakatani et al 2000**).

Flow cytometry analysis caused inhibition of the rate of liver cancer (HepG2) cell viability, it was necessary to assess cytotoxic effect of food additives on cell cycle arrest based cell cycle distribution. The results showed significant accumulation of HepG2 cells in G2/M phase, and confirmed that additives has cytotoxic effect via induction of G2/M phase arrest of the cell cycle (**Rashad et al., 2022**).

**Kocdor et al., (2015)** zinc showed cytotoxicity in p53-wild lung cancer cells but not in null cells at different supra physiological concentrations. Suggested that many cytotoxic molecules induce mitotic cell death (apoptosis) which occurs in parallel with G2/M arrest.

**Rashad et al., 2018** The quantitative real time-PCR was used to measure the mRNA levels of

*p53*, *Bax*, and *Bcl-2* genes. The data showed that food additives changed transcriptional levels of these related genes. The mRNA expression of *p53* and *Bax* were up-regulated, but, the transcription of *Bcl-2* was significantly down-regulated compared to the control.

According to the present data, ZnSO<sub>4</sub> led to *p53* activation and *Bcl-2* reduction which then activated mitochondria-mediated downstream molecular events including activation of caspase3. In conclusion, ZnSO<sub>4</sub> can effectively induce apoptosis of HepG2 cells. The induction of apoptosis by ZnSO<sub>4</sub> involved the activation of a mitochondria-mediated caspase cascade and the inhibition of the anti-apoptotic protein *Bcl-2*. Also ZnSO<sub>4</sub> at (50, 75, 100  $\mu$ g/ml) considered as cytotoxic for HepG2 cells but not for normal Wi-38, Higher than this concentration decreased cell viability in malignant and non-malignant cells as well as confirmed the occurrence of their cytotoxic effects.

#### 5. Conflicts of interest

“There are no conflicts to declare”.

#### 6. Acknowledgments

We sincerely thank the two anonymous reviewers for their helpful comments and their constructive feedback.

#### References

- [1] **Barbier O., Jacquillet G., Tauc M., Cougnon M., Poujeol P. (2005)**. Effect of heavy metals on, and handling by, the kidney. *Nephron Physiology*, 99, 105.
- [2] **Costello L.C. and Franklin R.B. (2016)**. A comprehensive review of the role of zinc in normal prostate function and metabolism; and its implications in prostate cancer. *Arch Biochem Biophys* 611:100– 112.  
<https://doi.org/10.1016/j.abb.2016.04.014>
- [3] **Cui, L., Schoene, N. W., Zhu, L., Fanzo, J. C., Alshatwi, A., and Lei, K. Y. (2002)**. Zinc depletion reduced Egr-1 and HNF-3 expression and apolipoprotein A-I promoter activity in HepG2 cells. *Am J Physiol Cell Physiol* 283: C623–C630.  
<https://doi.org/10.1152/ajpcell.00308.2001.-We>
- [4] **KLUG A. (2010)**: The discovery of zinc fingers and their applications in gene regulation and genome manipulation. *Annual Review in Biochemistry*, 79, 213-24.
- [5] **Kocdor H., Ates H., Aydin S., Cehreli R., Soyarat F., Kemanli P., Harmanci D., Cengiz H., and Kocdor MA., (2015)**: Zinc supplementation induces apoptosis and enhances antitumor efficacy

- of docetaxel in non-small-cell lung cancer. *Drug Design, Development and Therapy* 2015;9 3899–3909.
- [6] Livak, K. J., & Schmittgen, T. D. (2001). Analysis of relative gene expression data using real-time quantitative PCR and the  $2^{-\Delta\Delta C(T)}$  method. *Methods*, 25, 402–408.
- [7] Marcinčáková, D., Schusterová, P., Mudroňová, D., Csank, T., Falis, M., Fedorová, M., Marcinčák, S., Hus, K. K., and Legáth, J. (2019). Impact of zinc Sulphate exposition on viability, proliferation and cell cycle distribution of epithelial kidney cells. *Polish Journal of Environmental Studies*, 28(5), 3279–3286. <https://doi.org/10.15244/pjoes/94045>
- [8] McCord MC, Aizenman E (2018). The role of intracellular zinc release in aging, oxidative stress, and Alzheimer's disease. *Front Aging Neurosci* 6:1–16. <https://doi.org/10.3389/fnagi.2014.00077>
- [9] Nakatani T, Tawaramoto M, Opere Kennedy D, Kojima A, and Matsui-Yuasa I. (2000). Apoptosis induced by chelation of intracellular zinc is associated with depletion of cellular reduced glutathione level in rat hepatocytes. *Chem Biol Interact* 125: 151–163
- [10] Nazıroğlu M, Yürekli VA (2013): Effects of antiepileptic drugs on antioxidant and oxidant molecular pathways: focus on trace elements. *Cell Mol Neurobiol* 33:589–599
- [11] Plum, L. M.; Rink, L.; Haase, H. (2010): The essential toxin: Impact of zinc on human health. *International Journal of Environmental Research and Public Health*, 7 (4): 1342-365
- [12] Shima E. Rashad, Abdelhamid A. Haggrana, Ezzat I. Aboul-Elab, Ashraf H. Shaalanc, Ahmed Sabry S. Abdoond (2022). Cytotoxic and genotoxic effects of 50nm Gold Nanorods on mouse splenocytes and human cell lines. *Egypt. J. chem.*, Article in Press. [10.21608/EJCHEM.2022.134210.5914](https://doi.org/10.21608/EJCHEM.2022.134210.5914)
- [13] Shima E. Rashad, F. M. Abdel-Tawab, Eman M. Fahmy, Ashraf G. Attallah, Ekram S. Ahmed and A. A. Haggran (2018). Determination of genotoxic effects of some food additives on some human cancer cells by flow cytometry analysis. *Egypt. J. Genet. Cytol.*, 47:329-343.
- [14] Shima E. Rashad, F. M. Abdel-Tawab, Eman M. Fahmy, Ashraf G. Attallah, Ekram S. Ahmed and A. A. Haggran (2019). Assessment of genotoxic effects of some food additives on some human cancer cells. *AUJAS, Ain Shams Univ., Cairo, Egypt, Special Issue*, 27(1). DOI: [10.21608/AJS.2019.43668](https://doi.org/10.21608/AJS.2019.43668)
- [15] Shima E. Rashad\* 1, F. M. Abdel-Tawab 2, Eman M. Fahmy 2, Ashraf G. Attallah 1, Ekram S. Ahmed 1 and A. A. Haggran 1 (2021). Application of the yeast comet assay in testing some food additives for genotoxicity by comet assay in yeast. *Egypt. J. chem., Issue*, 64: (12) 7649-7667. [10.21608/EJCHEM.2021.90428.4315](https://doi.org/10.21608/EJCHEM.2021.90428.4315)
- [16] Silvera SAN, Rohan TE (2007): Trace elements and cancer risk: a review of the epidemiologic evidence. *Cancer Causes Control*, 18:7–27
- [17] Sliwinski, t.; czechowska, a.; kolodziejczak, m.; jajte, j.; jarosinska, m. W.; blasiak, j. (2009): Zinc salts differentially modulate DNA damage in normal and cancer cells. *Cell Biology International*, 33(4): 542-547.
- [18] Vermes, I., Haanen, C., Steffens-N., H., Reutelingsperger, C., (1995). A novel assay for apoptosis Flow cytometric detection of phosphatidylserine expression on early apoptotic cells using fluorescein labelled Annexin V. *Journal of Immunological Methods*, 184 (1), 39-51.
- [19] Wang, Y. H., Li, K. J., Mao, L., Hu, X., Zhao, W. J., Hu, A., and Zheng, W. J. (2013): Effects of exogenous zinc on cell cycle, apoptosis and viability of MDAMB231, HepG2 and 293 T cells. *Biological Trace Element Research*, 154(3), 418–426. <https://doi.org/10.1007/s12011-013-9737-1>
- [20] Wang, Y. hong, Zhao, W. jie, Zheng, W. juan, Mao, L., Lian, H. zhen, Hu, X., & Hua, Z. chun. (2016): Effects of Different Zinc Species on Cellular Zinc Distribution, Cell Cycle, Apoptosis and Viability in MDAMB231 Cells. *Biological Trace Element Research*, 170(1), 75–83. <https://doi.org/10.1007/s12011-015-0377-5>
- [21] Xie H, Holmes AL, Young JL et al (2009): Zinc chromate induces chromosome instability and DNA double strand breaks in human lung cells. *Toxicol App Pharmacol* 234:293–299
- [22] Yehy.h., lee y.t., hsiehy.l., and hwangd.f. (2011): Dietary taurine reduces zinc-induced toxicity in male wistar rat. *Journal of Food Science*, 76, T90-T98.
- [23] Yuan, N., Wang, Y. H., Li, K. J., Zhao, Y., Hu, X., Mao, L., and Zheng, W. J. (2012): Effects of exogenous zinc on the cellular zinc distribution and cell cycle of A549 cells. *Bioscience, Biotechnology and Biochemistry*, 76(11), 2014–2020. <https://doi.org/10.1271/bbb.120216>
- [24] Zaman, M., Johnson, A., Petersingham, G., Muench, G., Dong, Q., and Wu, Ming. (2019). Protein kinase CK2 is involved in zinc homeostasis in breast and prostate cancer cells. *BioMetals*. 32. [10.1007/s10534-019-00218-z](https://doi.org/10.1007/s10534-019-00218-z).
- [25] Zhang X., Wang Z., Mao L., Dong X., Peng Q., Chen J., Tan C., Hu R. (2017): Effect of ZnO

nanoparticle on cell viability, zinc uptake efficiency, and zinc transporters gene expression: a comparison with ZnO and ZnSo<sub>4</sub>. *Czech J. Anim. Sci.*, 62, 32–41

[26] Zhao, W. J., Song, Q., Zhang, Z. J., Mao, L., Zheng, W. J., Hu, X., & Lian, H. (2015): The kinetic response of the proteome in A549 cells exposed to ZnSo<sub>4</sub> stress. *PLoS ONE*, 10(7), 1–21.

<https://doi.org/10.1371/journal.pone.0133451>

[27] Zodl b., zeiner m., sargazi m., robertsn.b., marktl w., steffani., ekmekcioglu c (2003). Toxic and biochemical effects of zinc in CaCo-2 cells. *Journal of Inorganic Biochemistry*, 97, 324-3



